EPRG-PRCI-APGA
23rd Joint Technical Meeting
Edinburgh, Scotland
6–10 June 2022

EPRG-PRCI-APGA
23rd Joint Technical Meeting
Edinburgh, Scotland • 6–10 June 2022

THE DECOMPRESSED STRESS LEVEL IN DENSE PHASE CARBON DIOXIDE FULL-SCALE FRACTURE PROPAGATION TESTS
PAPER 11

Andrew Cosham*
Ninth Planet Engineering, Newcastle upon Tyne, UK

Guillaume Michal
University of Wollongong, Wollongong, NSW, Australia

Erling Østby
DNV, Høvik, Norway

Julian Barnett
National Grid Ventures, Solihull, UK

* presenting author

ABSTRACT

Full-scale fracture propagation tests with liquid or dense phase carbon dioxide (CO_2) have been conducted by four research projects: CO2PIPETRANS, COOLTRANS, SARCO2B and CO2SafeArrest. A total of nine full-scale tests have been conducted, in 406.4, 610.0 and 914.0 mm outside diameter, Grade L415 and L450 line pipe.

COOLTRANS and CO2SafeArrest have collaborated in a reanalysis of the raw pressure transducer and timing wire data from each of their respective full-scale tests, and an exchange of the (previously unpublished) calculated decompressed stress levels. The data from the timing wires immediately upstream and downstream of each pressure transducer is used to identify the relevant data recorded by the pressure transducer. The pressure at the crack tip is then taken to be the mean recorded between the times when the leading and trailing timing wires broke.

A re-plotting of these data points confirms the appropriateness of the empirical model in DNV-RP-F104. It also provides an insight into a possible difference between the effective crack length for natural gas, and for liquid or dense phase CO_2.

DISCLAIMER

1. INTRODUCTION

A simple empirical model for the design of a pipeline transporting CO_2 to arrest a running ductile fracture is presented in 5.6.5 *Procedure for evaluating ductile fracture propagation control* of DNV-RP-F104 September 2021 *Design and operation of carbon dioxide pipelines* [1]. The model is expressed in terms of a plot of the normalised decompressed stress level and the normalised toughness (see Figure 5-3 of DNV-RP-F104). A plot of the normalised decompressed stress level and the normalised toughness is based on Figure J-12 of Maxey, 1974 [2]. Equation (D.1) in Annex D of BS ISO 27913 [3] is also based on Figure J-12. Figure J-12 summarises the development of the arrest stress level, a part of the Two Curve Model.

The normalised toughness is a function of the Charpy V-notch impact energy, the yield strength, and the radius and wall thickness of the pipe.

The normalised decompressed stress level is a function of the hoop stress at the crack tip and the yield strength. The hoop stress at the crack tip is a notional term; it is simply the pressure at the crack tip multiplied by the ratio of the radius to the wall thickness of the pipe, i.e. $p(R/t)$.

The test section in a full-scale fracture propagation test is instrumented with fast-response pressure transducers and timing wires. The pressure at the crack tip can be estimated using the data recorded by the pressure transducers and the timing wires.

COOLTRANS and CO2SafeArrest have collaborated in a reanalysis of the raw pressure transducer and timing wire data from each of their respective full-scale tests, and an exchange of the (previously unpublished) calculated decompressed stress levels.

2. THE TWO CURVE MODEL

The Two Curve Model is a semi-empirical model developed by the Battelle Columbus Laboratories in the early 1970s, see Maxey et al., 1972, 1973 [4,5] and Maxey, 1974 [2]. It describes the relationship between the speed of the decompression wave and the speed of the ductile fracture. The Two Curve Model is a decompression curve and a fracture curve.

The decompression curve for CO_2 in the liquid or dense phase exhibits a long plateau[1,2]. It has therefore become common to (conservatively) simplify the application of the Two Curve Model, reducing the curves to a saturation pressure and an arrest pressure, as originally noted in King, 1982 [6,7], Maxey, 1986 [8] and Rothwell, 1988 [9]. A running fracture will propagate if the saturation pressure is greater than or equal to the arrest pressure. It will arrest if the saturation pressure is less than the arrest pressure.

A brief digression into the derivation of the Two Curve Model is warranted because it highlights the relevance of Figure J-12, the plot of the normalised decompressed stress level and the normalised toughness, and it introduces the equation for the arrest stress and the effective crack length:

Maxey et al., 1972, 1973 [4,5] considered an arrested crack to be different from initiation only in that it is a longer crack at a lower stress level, and therefore that the description of the role of geometry in the

[1] The initial pressure and initial temperature, and composition, define whether the decompression path passes through the liquid phase and intersects the bubble point curve, or through the vapour phase and intersects the dew point curve. The plateau is long if the decompression path passes through the liquid phase.

[2] An isentropic decompression model predicts a discontinuity at the point where the decompression path intersects the bubble or dew point curves. The decompression curve exhibits a plateau. The decompression curve constructed from the pressure transducers in a full-scale fracture propagation test or a shock tube test exhibits a sloping plateau; the pressure at the end of the plateau is lower than that at the start of the plateau.

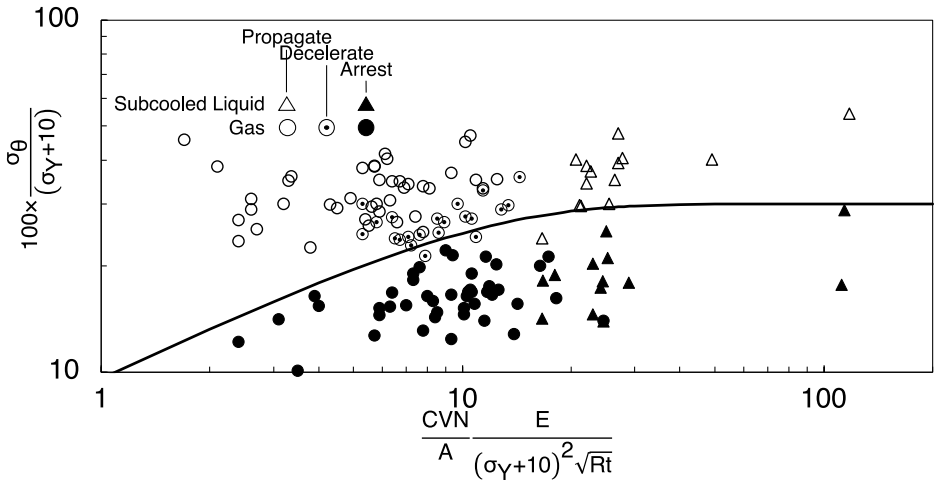

Figure 1 A plot of the normalised decompressed stress level versus the normalised toughness for the full-scale tests conducted with natural gas or a subcooled liquid tabulated in Appendix II of Maxey et al., 1972 [4], and the arrest stress level calculated using an effective length, $2c/(Rt)^{0.5}$, equal to 6.0 … cf. Figure J.12 *Determination of the Arrest Stress Level* of Maxey, 1974 [2]

initiation of a through-wall crack is relevant to the arrest of a fracture. A maximum effective crack length was considered to represent steady-state ductile fracture propagation.

Maxey, 1972 [4] described the initiation, propagation and arrest of a ductile fracture as follows:

1. Initiation.
2. The crack lengthens and correspondingly *M* [the Folias factor] increases and the fracture velocity increases through some supercritical zone of acceleration. The internal gas pressure will momentarily remain the same, as the full opening necessary for outflow of the gas has not yet been established.
3. It is assumed that some maximum effective crack length ($2c/(Rt)^{0.5}$) and the corresponding *M* value is achieved.
4. At this point, a full opening develops and decompression starts so that the internal pressure and corresponding [hoop stress] drops. The level to which the pressure drops will depend upon the fracture speed.
5. Arrest will occur if the decompressed level is within the decelerate zone and if the zero speed stress level is beneath the initiation curve.

Arrest Stress Level A ductile fracture is assumed not to propagate if the local stress level is less than the arrest stress level. It was shown that a normalised effective crack length that separated the arrest and propagate data points could be defined on a plot of the normalised decompressed stress level versus the normalised toughness, as shown in Figure 1, a replot of Figure J-12 of Maxey, 1974 [2]. The line dividing the decelerate (or arrest) and the propagate zones is described by Equation (1) (a log-secant (ln-sec) equation), with $2c/(Rt)^{0.5}$ equal to 6.0 and *M* equal to 3.33[3]. *M* is a factor (or correction) that represents the additional stress concentration at the crack tip of a longitudinally orientated through-

[3] Folias, 1965 [10] presents the integral equations for the stress field around a longitudinally orientated through-wall crack in cylinder, and a closed-form analytical solution that is valid for short cracks. Erdogan & Kibler, 1969 [11] present a numerical solution to these integral equations, tabulated in Table 1 of Erdogan & Kibler, 1969. Figure 1 *Relationship between the bulge stress concentration, M_T, and the flaw and pipe geometries* of Maxey et al., 1972 and Figure J-3 *Relationship between the Folias correction and the flaw and pipe geometries* of Maxey, 1974 plot the results of this numerical solution. Figure J-3 of Maxey, 1974 also includes an equation "for computer computations" that approximates the numerical solution. The value of *M* for $2c/(Rt)^{0.5}$ equal to 6.0 is 3.3079, calculated using the numerical solution, and 3.3469, calculated using the approximate equation. Maxey, et al., 1972 (and Maxey, 1974) quote *M* equal to 3.33.

wall crack in cylinder relative to a through-wall crack in a flat plate caused by the bulging of the cylinder due to the internal pressure.

Equation (1) is based on a plasticity correction to linear-elastic fracture mechanics derived from the crack tip opening displacement, described in Hahn et al., 1969 [12] (and is equivalent to the Bilby-Cottrell-Swindon Dislocation Model (the collapse modified strip-yield model), as described in Heald et al., 1963 [13,14]). The flow stress was defined empirically, with reference to burst tests on through-wall defects. The Folias factor is based on linear-elastic theory. The effective crack length, $2c/(Rt)^{0.5}$, is equal to 6.0. It is empirical.

The full-scale fracture propagation test data plotted in Figure 1, from Appendix II of Maxey et al., 1973 [5], is representative of typical line pipe steels, both semi and fully-killed, of Grades X52 through to X70 (with a handful of an experimental Grade X100), produced prior to 1973, in outside diameters up to and including 1066.8 mm (42"), and diameter to wall thickness ratios that range from 13.8 to 113.2. The full-size equivalent, upper-shelf Charpy V-notch impact energies of the data range from 20 to 159 J, and are typically less than approximately 70 J.

The arrest stress level (the decompressed stress level at arrest) is Equation (2), which is Equation (1) rearranged in terms of the upper shelf Charpy V-notch impact energy, the flow stress and the geometry (the radius and the wall thickness).

$$\frac{K^2}{\bar{\sigma}^2\sqrt{Rt}} = CVN\frac{12}{A}E\frac{1}{\bar{\sigma}^2\sqrt{Rt}} = \frac{4}{\pi}\frac{2c}{\sqrt{Rt}}\ln\sec\left(\frac{\pi}{2}M\frac{\sigma_\theta}{\bar{\sigma}}\right) \tag{1}$$

$$\sigma_\theta = \frac{\bar{\sigma}}{M}\frac{2}{\pi}\operatorname{acos}\left[\exp\left(-CVN\frac{12}{A}E\frac{\pi}{\bar{\sigma}^2\sqrt{Rt}}\left(\frac{1}{4}\frac{\sqrt{Rt}}{2c}\right)\right)\right]$$
$$= \frac{\bar{\sigma}}{3.33}\frac{2}{\pi}\operatorname{acos}\left[\exp\left(-CVN\frac{12}{A}E\frac{\pi}{\bar{\sigma}^2\sqrt{Rt}}\frac{1}{24}\right)\right] \tag{2}$$

3. CO2PIPETRANS, COOLTRANS, SARCO2B AND CO2SAFEARREST

Full-scale fracture propagation tests with liquid or dense phase CO_2 have been conducted by four research projects: CO2PIPETRANS, COOLTRANS, SARCO2B and CO2SafeArrest [15-25]. A total of nine (9) full-scale tests have been conducted, as summarised in Table 1[4]. The number of tests is relatively small; in comparison, over one hundred full-scale fracture propagation tests with lean or rich natural gas have been conducted. The tests for COOLTRANS and CO2SafeArrest were conducted by the Spadeadam Testing and Research Centre, DNVGL. The tests for SARCO2B were conducted by Centro Sviluppo Materiali.

CO2PIPETRANS 1	406.4x6.2-12.7 mm, Grades X60 (L415) & X65 (L450), HFI & SMLS	[## June 2012]
CO2PIPETRANS 2	406.4x6.2-12.7 mm, Grades X60 (L415) & X65 (L450), HFI & SMLS	[## June 2012]
COOLTRANS Test 01	914.0x25.4 mm, Grade L450, SAWL	[21 April 2012]
COOLTRANS Test 02	914.0x25.4 mm, Grade L450, SAWL	[13 October 2012]
COOLTRANS Test 03	610.0x19.1 mm, Grade L450, SAWL	[25 July 2015]
SARCO2B 1	610.0x12.7-13.7 mm, Grade L450, HFI & SAWL	[11 February 2015]
SARCO2B 2	610.0x12.5-13.7 mm, Grade L450, HFI & SAWL	[14 April 2016]
CO2SafeArrest 1	610.0x13.5-15.0 mm, Grade L450, SAWL	[30 September 2017]
CO2SafeArrest 2	610.0x14.5 mm, Grade L450, SAWL	[24 March 2018]

Table 1 Full-scale fracture propagation tests conducted using liquid or dense phase CO_2

[4] A further three tests were conducted in the early 1980s to investigate the effectiveness of mechanical crack arrestors. One test on 323.9x5.7 mm, Grade X65 line pipe is described in Maxey, 1983 [26] and Wilkowski et al., 2006 [27], and two tests on 508x7.62, Grade X52 and 11.13 mm, Grade X70 line pipe are described in Ahluwalia & Gupta, 1985 [28].

The two full-scale tests conducted for CO2PIPETRANS, by SINTEF, are significantly different from the other seven tests, in that the test rig was relatively short (approximately 24 m long) and the reservoirs were not anchored with reinforced concrete anchor blocks and buried[5].

4. DNV-RP-F104 SEPTEMBER 2021

A simple empirical model for the design of a pipeline transporting CO_2 to arrest a running ductile fracture is presented in 5.6.5 *Procedure for evaluating ductile fracture propagation control* of DNV-RP-F104 [1], see Figure 5-3 Sch*eme for evaluation of running ductile fracture arrest in dense CO_2 pipelines*, and Table 5-4 *Evaluation of assessment results* and Table 5-5 *Limitations of the assessment model*, repeated in Table 2 and Table 3. It is described in more detail in Michal et al., 2020 [25]. The model was developed under the CO2SafeArrest joint industry project, led by DNV, Norway and the Energy Pipelines Collaborative Research Centre, Australia.

The simple empirical model is based on Figure J-12 of Maxey, 1974 [2]. Figure J-12 is a plot of the normalised decompressed stress level versus the normalised toughness. The normalised decompressed stress level is the normalised hoop stress corresponding to the (estimated) pressure at the crack tip. Michal et al., 2020 estimated the pressure at the crack tip in each test pipe in the nine full-scale fracture propagation tests (see Table 1). The pressure at the crack tip tabulated in Table 3 of Michal et al., 2020 is either based on the raw data recorded by the respective pressure transducers and timing wires, or where the raw data was not available (as for COOLTRANS Tests 01, 02 and 03 and SARCO2B Tests 1 and 2), on the test data reported in the published literature.

The empirical boundary was derived on the basis that an arrest point defines the conditions for arrest to the right and below the point and that a propagate point defines the conditions for propagation to the left and above the point. Figure 5-3 denotes “Propagation expected”, “Evaluation based on special assessments” and “Evaluation based on small-scale testing”. “Evaluation based on small-scale testing” is the “Arrest region” in Michal et al., 2020.

The arrest region is bounded by Pipe 3W in COOLTRANS Test 01 and Pipe 4W in CO2SafeArrest 2[6]. The empirical boundary is intended to be conservative.

The empirical model, as defined in Figure 5-3 and Table 5-4, is plotted in Figure 2. Also plotted (as a dashed line) is the “Possible boundary extension, no supporting test data” indicated in Figure 3 of Michal et al., 2020, but not in Figure 5-3 of DNV-RP-F104[7,8].

The simple empirical model equates to a limit on the abscissa (the horizontal axis) and a limit on the ordinate (the vertical axis). It limits the ordinate (the vertical axis) to 0.27, compared with approximately 0.30 for the Two Curve Model and approximately 0.25 for Annex D of BS ISO 27913.

Figure 5-3 is more conservative than Annex D of BS ISO 27913 at lower values of the normalised toughness. Annex D is more conservative than Figure 5-3 at higher values of the normalised toughness. Annex D is non-conservative with respect to some of the full-scale test data at lower values of the normalised toughness, see Figure 2.

[5] CO2PIPETRANS 1 and 2 do not bound the arrest or propagate data points, so their inclusion (or exclusion) is not significant.

[6] The west side of CO2SafeArrest 2 was partially exposed, with no backfill over the upper quadrant of the pipe (between approximately 10 and 2 o’clock). The ordinates of the arrest points for Pipes 4E and 4W in CO2SafeArrest 2 are very similar.

[7] It is a straight line from (0, 0) to (25, 0.23).

[8] Figure 5-3 of DNV-RP-F104 is slightly different to Figure 3 of Michal et al., 2020. The abscissa (the horizontal axis) in Figures 3 and 5-3 differ by a factor of $\pi/24$, and the coordinates of the empirical boundary have been rounded-up (so Figure 5-3 is slightly more conservative than Figure 3).

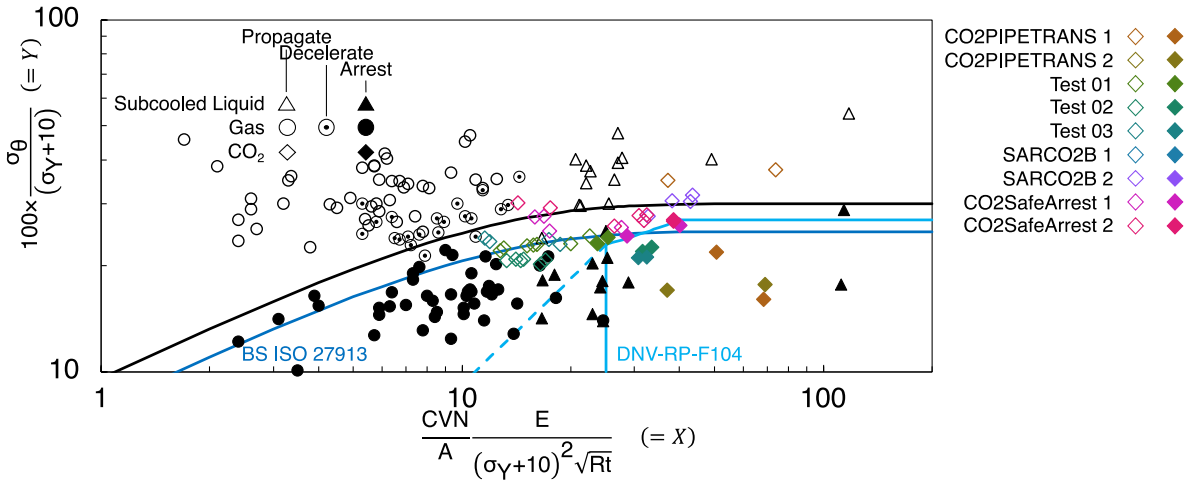

Figure 2 A plot of the normalised decompressed stress level (=*Y*) versus the normalised toughness (=*X*) for the full-scale tests conducted with carbon dioxide, and the modified Two Curve Model in Annex D of BS ISO 27913 and the simple empirical model in Figure 5-3 of DNV-RP-F104 … cf. Figure 3: *Experimental data points reported in the plan of the non-dimensional fracture resistance and non-dimensional driving force* of Michal et al., 2020 [25], and Figure 5-3 *Scheme for evaluation of running ductile fracture arrest in dense CO_2 pipelines* of DNV-RP-F104

X	*Y*	Conclusions
For $X < 25$ or design parameters outside limits defined in Table 5-5	$Y \leq 0.23$	Special assessments are required.
	$Y > 0.23$	Crack propagation judged likely. Re-design, potentially including qualification of crack arrestors, necessary.
For $25 \leq X < 40$	$Y \leq 0.23 + 0.00267\times(X-25)$ and design parameters within limits defined in Table 5-5	Crack arrest judged likely without any further precautions.
	$Y > 0.23 + 0.00267\times(X-25)$	Crack propagation judged likely. Re-design, potentially including qualification of crack arrestors, necessary.
For $X \geq 40$	$Y \leq 0.27$ and design parameters within limits defined in Table 5-5	Crack arrest judged likely without any further precautions.
	$Y > 0.27$	Crack propagation judged likely. Re-design, potentially including qualification of crack arrestors, necessary.

Table 2 … cf. Table 5-4 *Evaluation of assessment results* of DNV-RP-F104

Table 5-5 *Limitations of the assessment model* (see Table 3) of DNV-RP-F104 limits the application of Figure 5-3 to 406.4-914.4 mm (16.0-36.0") outside diameter, 10-26 mm wall thickness and API Spec 5L X60 and X65, and a full-size equivalent CVN impact energy greater than or equal to 250 J. It also limits it to submerged arc welded line pipe fabricated using thermomechanical controlled processed steel. Table 5-5 is (intentionally) quite restrictive, but it simply reflects the range of the nine full-scale tests that have been conducted.

Limitation	Comment
Characteristic CVN energy: 250 J or above	Crack arrest in large-scale test has only been observed in base material pipes with CVN energy of approximately 300 J or higher. For lower CVN energy values there are indications that the governing fracture mechanisms can be different from the observed mechanisms in pipes where arrest have been observed (Davis et. al., 2020). A basis for using the simplified model is that the governing failure mechanisms should be similar to the ones observed in the large-scale tests which are used in the development of the model. This is currently taken to likely being fulfilled if the CVN energy is 250 J or higher.
Pipeline outer diameter, D: 16" to 36"	The range of applicable pipeline diameters corresponds to the range considered in large-scale test campaigns.
Pipeline wall thickness, t: 10 mm to 26 mm	The range of applicable wall thicknesses is based on the wall thickness range considered in large-scale test campaigns used as basis for the simplified model, with some extrapolation to smaller wall thicknesses.
Pipes grades: X60 to X65	This covers the primary grades used in large-scale testing.
C-Mn submerged arc-welded TMCP pipes	The available large-scale test data are obtained for submerged arc-welded TMCP pipes. HFW pipes are currently not considered to be covered by criteria due to the possibility of the pipes having high Y/T ratios, and uncertainties associated the impact of this on the arrest capability of the pipes. The differences in alloying philosophy and microstructure for QT or seamless pipes renders the applicability of the defined criteria uncertain for these pipes. However, it is likely that acceptable solutions can be demonstrated by special considerations for high quality QT or seamless pipes.
Pipeline content: fluids containing overwhelmingly CO_2	
Backfill conditions: no specific restrictions	There are few results considering the effect of backfill on running ductile fracture in CO_2 pipelines. The few results that exist point to backfill having an effect on the crack velocity, but potentially less on the pipe properties leading to arrest.

Table 3 … cf. Table 5-5 *Limitations of the assessment model* of DNV-RP-F104

5. AN ESTIMATE OF THE DECOMPRESSED STRESS LEVEL

COOLTRANS and CO2SafeArrest have collaborated in a reanalysis of the raw data from each of their respective full-scale fracture propagation tests. The raw data recorded by the fast-response pressure transducers and the timing wires in the COOLTRANS Tests 01, 02 and 03, and CO2SafeArrest Tests 1 and 2 have been reanalysed in order to obtain a revised estimate of the pressure at the tip of the propagating fracture (the pressure at the crack tip).

The test section in a full-scale test is instrumented with fast-response pressure transducers and timing wires. Timing wires are installed along the test section at intervals of approximately 1.0 m. One or two (typically two) pressure transducers are installed in each test pipe. The pressure transducers are installed approximately equidistant between the adjacent pairs of timing wires. The pressure

transducers record the propagation of the expansion wave. The timing wires record the propagation of the fracture.

The pressure at the crack tip is estimated using the pressure transducers and the timing wires. The relevant data recorded by a pressure transducer is identified using the time when the leading and trailing timing wires broke on either side of the pressure transducer. The timing wires break at or before the arrival of the crack tip; the ovalisation of the pipe ahead of the crack tip might be sufficient to break a timing wire and movement of the pipe might be sufficient to break the cabling. The timing wires that appear (qualitatively) to be outliers (so, broke too early) and were not used to estimate the speed of the fracture, have also not been used to bound the data recorded by the pressure transducers.

The pressure at the crack tip is taken to be the mean of the data recorded by the pressure transducer between the times when the leading and trailing timing wires broke.

A number of pressure transducers stopped recording data before the leading timing wire broke or after the leading and before the trailing timing wire broke, or recorded data behind the crack tip[9]. The mean of the data recorded in the five milliseconds (an arbitrary value) before the pressure transducer stopped recording data is used when it stopped recording data before the leading timing wire broke. The mean of the data recorded between the time when the leading timing wire broke and the time halfway between the times when the leading and trailing timing wires broke, or the mean of the data recorded between the time when the leading timing wire broke and the time when the pressure transducer recorded a significant decrease in pressure, is used when it stopped recording data after the leading timing wire broke or when it (appeared to have) recorded data behind the crack tip.

The estimated pressure at the crack tip is tabulated in Tables 4 and 5. The timing wires used in the estimation of the pressure are also indicated.

The diameter, wall thickness, average measured yield and tensile strengths and full-size equivalent Charpy V-notch impact energy that have been used to calculate the normalised decompressed stress level and the normalised toughness are also tabulated. The yield and tensile strengths are the values that were determined using flattened strap (rectangular) specimens. The radius of the striker used in the Charpy V-notch impact tests (8 or 2 mm as per ASTM E23 [29] and BS EN ISO 148-1 [30]) is indicated.

The mechanical properties were measured at each end of each pipe (designated North or South). Tables 4 and 5 tabulate the data for each end of each pipe. Table 3 of Michal et al., 2020 tabulates the data for each pipe.

5.1. COOLTRANS Tests 01, 02 and 03 (see Table 4)

The initiation pipe in Tests 01, 02 and 03 did not contain any pressure transducers. The estimated pressures are those from the pressure transducers in the next pipes.

No. 02 in Test 01 did not record data. The estimated pressure is that from No 01, the other pressure transducer in the pipe.

The pressure transducers on the east side of Test 02 did not record data. The estimated pressures on the east side are assumed to be equal to those on the west side.

5.2. CO2SafeArrest Tests 1 and 2 (see Table 5)

The initiation pipes in Tests 1 and 2 contained one pressure transducer at one end of the pipes. The estimated pressures at the other end of the pipes are those from these pressure transducers.

[9] A pressure transducer might or might not record what appears to be reliable data, see Figs. 8 and 9 of Cosham et al., 2014 [17], Fig 11 of Cosham et al, 2016 [18], Fig. 10 of Michal et al., 2018 [23] and Figure 14 of Michal et al., 2019 [24].

Designation	Pipe No.	diameter, mm	wall thickness, mm	average yield strength, N.mm^{-2}	average tensile strength, N.mm^{-2}	average CVN impact energy, J [2 mm]	[8 mm]	pressure, barg	Arrest or Prop.			
3W	26N	914.0	25.4	507.0	596.0	330.5	-	75.7	A	16	82-83	[5 ms]
	26S	914.0	25.4	484.5	582.0	302	-	75.8	P	15	77-79	[5 ms]
2W	47N	914.0	25.4	509.5	627.5	272.5	-	71.0	P	14	70-72	
	47S	914.0	25.4	483.33	606.33	258.5	-	76.7	P	13	65-67	[5 ms]
1W	44N	914.0	25.4	504.5	615.5	226	-	70.8	P	12	59-61	
	44S	914.0	25.4	498.5	616.5	201	-	73.8	P	11	55-59	[5 ms]
initiation	32S	914.0	25.4	511.0	633.0	183	-	73.8	P			
	32N	914.0	25.4	522.5	639.0	186	-	73.4	P			
1E	41S	914.0	25.4	496.5	612.5	213	-	73.4	P	01	07-08	
	41N	914.0	25.4	511.5	622.0	201.5	-	73.4	P	02		[no data]
2E	42S	914.0	25.4	495.0	613.0	207	-	73.9	P	03	18-19	[5 ms]
	42N	914.0	25.4	499.0	614.0	223.5	-	71.2	P	04	23-24	[5 ms]
3E	48S	914.0	25.4	456.0	581.5	273	-	72.5	P	05	29-30	[5 ms]
	48N	914.0	25.4	477.0	598.0	267.33	-	74.1	P	06	34-35	[5 ms]
4E	25S	914.0	25.4	475.5	576.5	292	-	71.4	A	07	37-40	[5 ms]
3W	13N	914.0	25.4	445.0	538.0	388	-	62.0	A			
2W	44996N	914.0	25.4	496.5	588.0	227.33	-	62.0	P			
	44996S	914.0	25.4	496.0	627.0	230	-	62.0	P	06	33-38	
1W	62S	914.0	25.4	491.5	612.0	212	-	62.0	P	05	30-32	
	62N	914.0	25.4	498.5	612.0	179	-	60.8	P	04	26-27	
initiation	34N	914.0	25.4	499.0	618.5	179	-	60.8	P			
	34S	914.0	25.4	495.0	613.5	187	-	60.8	P			
1E	61N	914.0	25.4	501.0	619.0	191	-	60.8	P	01		[no data]
	61S	914.0	25.4	502.5	617.5	203	-	62.0	P	02		[no data]
2E	43S	914.0	25.4	506.0	627.5	217	-	62.0	P			
	43N	914.0	25.4	518.0	617.0	246	-	62.0	P	03		[no data]
3E	14S	914.0	25.4	481.0	557.5	355.67	-	62.0	A			
2W	65N	610.0	19.6	522.0	597.0	342	-	85.5	A	12	55-56	[5 ms]
1W	78N	610.0	19.1	477.0	590.5	152	-	83.2	P	11	50-51[2]	[5 ms]
	78S	610.0	19.1	473.0	586.0	152.33	-	80.6	P	10	43-44[1]	
initiation	2A	610.0	19.4	462.0	582.0	97	-	80.6	P			
	2B	610.0	19.3	477.5	572.0	106.33	-	83.2	P			
1E	81S	610.0	19.2	494.0	607.0	171.67	-	83.2	P	01	06-09[2]	
	81N	610.0	19.2	486.5	592.0	173.89	-	82.9	P	02	12-15[2]	[5 ms]
2E	66N	610.0	19.5	528.0	608.0	328.33	-	82.7	A	03	16-##	

Notes:

1. The estimated pressure is the mean of the data recorded between the time when the leading timing wire broke and the time halfway between the times when the leading and trailing timing wires broke.
2. The estimated pressure is the mean of the data recorded between the time when the leading timing wire broke and the time when the pressure transducer recorded a significant decrease in pressure.

Table 4 The diameter, wall thickness, average measured yield and tensile strength, full-size equivalent CVN impact energy, and the estimated pressure at the crack tip for COOLTRANS Tests 01, 02 and 03

Designation	Pipe No.	diameter, mm	wall thickness, mm	average yield strength, N.mm^{-2}	average tensile strength, N.mm^{-2}	average CVN impact energy, J [2 mm]	[8 mm]	pressure, barg	Arrest or Prop.			
3W	N	610.0	13.7	503.0	612.0	-	436	67.8	A	15	62-##	[5 ms]
	S	610.0	13.6	459.0	584.0	302	438	65.0	P	14	61-62[1]	
2W	N	610.0	13.5	517.0	631.0	143	218	64.8	P	13	56-57[1]	
	S	610.0	13.6	493.0	612.0	-	268	65.5	P	12	51-52[1]	
1W	S	610.0	13.4	438.0	606.0	107	130	63.9	P	11	46-47[1]	
	N	610.0	13.4	463.0	619.0	-	110	63.9	P			
1E	S	610.0	13.4	449.0	620.0	-	112	62.1	P			
	N	610.0	13.5	457.0	602.0	114	116	62.1	P	01	05-06[1]	
2E	S	610.0	13.6	475.0	611.0	-	422	65.0	P	02	10-11[1]	
	N	610.0	13.6	505.0	616.0	215	199	66.1	P	03	15-16	[5 ms]
3E	S	610.0	13.6	509.0	619.0	247	419	64.5	A	04	19-##	[5 ms]
4W	N	610.0	15.0	502.0	603.0	-	445	79.0	A	23	69-##	[5 ms]
	S	610.0	15.0	465.0	579.0	308	439	78.5	P	22	65-66[1]	
3W	S	610.0	15.0	508.0	616.0	238	340	74.0	P	21	61-62	
	N	610.0	15.0	507.0	615.0	222	338	74.7	P	20	56-57	
2W	N	610.0	14.7	492.0	599.0	262	331	74.6	P	18	51-52[1]	
	S	610.0	14.7	463.0	589.0	242	266	74.4	P	16	46-47[1]	
1W	N	610.0	14.7	458.0	611.0	99	117	76.0	P	15	41-42[1]	
	S	610.0	14.7	445.0	604.0	-	122	76.0	P			
1E	S	610.0	14.7	457.0	616.0	-	110	75.0	P			
	N	610.0	14.6	450.0	601.0	-	135	75.0	P	01	05-06[1]	
2E	S	610.0	14.7	463.0	576.0	-	254	75.6	P	03	09-12	
	N	610.0	14.7	494.0	599.0	-	357	76.3	P	06	15-16	
3E	N	610.0	14.7	492.0	606.0	-	330	77.1	P	08	20-21	
	S	610.0	14.7	501.0	611.0	-	378	75.8	P	09	25-26[1]	
4E	N	610.0	15.0	478.0	580.0	-	441	76.4	A	10	29-30[2]	[5 ms]

Table 5 The diameter, wall thickness, average measured yield and tensile strength, full-size equivalent CVN impact energy, and the estimated pressure at the crack tip for CO2pipetrans Tests 01 and 02

The estimated pressures at the crack tip, see Tables 4 and 5, are variously slightly higher or lower than those reported in Table 3 of Michal et al., 2020, with, on average, the data points for the COOLTRANS Tests 01, 02 and 03 moving down slightly and the data points for the CO2SafeArrest Tests 1 and 2 moving up slightly (and more so for Test 2 than Test 1) when plotted as per Figure 3 of Michal et al., 2020, as evident in a comparison of Figures 2 and **3**. A conservative estimate would underestimate the pressure at the crack tip (moving the data points down).

The empirical boundary in Figure 5-3 of DNV-RP-F101 (and in Figure 3 of Michal et al., 2020) is still conservative; all of the propagate data points fall outside of the area demarked by the empirical criterion as arrest ("Arrest region" or "Evaluation based on small-scale testing"), see Figure 3. A number of propagate data points from the CO2SafeArrest Tests 1 and 2 do fall inside the area if the Charpy V-notch impact energy measured using an 8 mm striker is used (the impact energy measured using the 8 mm striker was generally higher than that measured using the 2 mm striker, see Table 5). However, it is important to note that Table 5-3 of DNV-RP-F101 states that Charpy V-notch tests should be conducted using the 2 mm striker geometry that is described in ISO 148-1.

The reanalysis of the data points confirms the appropriateness of Figure 5-3. The empirical boundary is conservative using the estimated pressures in Tables 4 and 5, or in Table 3 of Michal et al., 2020.

6. A MODIFIED TWO CURVE MODEL WITH A LONGER EFFECTIVE LENGTH

The Two Curve Model assumes an effective normalised crack length, $2c/(Rt)^{½}$, equal to 6.0. The results of the full-scale fracture propagation tests that have been conducted with liquid or dense phase CO_2 indicate that either the driving force is higher and/or that the resistance is lower than expected. The unmodified (or uncorrected) Two Curve Model is non-conservative, see Figure 2. The empirical correction factors on the Charpy V-notch impact energy are also not sufficient to correct the non-conservatism. It is also of note, but might simply be coincidental, that the propagate data points from the tests with sub-cooled liquid tend to lie closer to the line than the tests with gas, and that one propagate data point lies below the line (two 'decelerate' points also lie below the line). The decompression behaviour of a sub-cooled liquid is similar to that of liquid or dense phase CO_2 (the decompression path is through the liquid phase).

A higher driving force and/or a lower resistance (for whatever reason) is represented by increasing the effective length. The effect of increasing the effective length to 8.0 is illustrated in Figure 3. M is equal to 4.1645 (calculated using the numerical solution tabulated in Table 1 of Erdogan & Kibler, 1969 [11]). The increase in the effective length is approximately analogous to a factor on the ordinate and on the abscissa (cf. Annex D of BS ISO 27913); a longer effective length is a more appropriate modification because it, in effect, corrects both the abscissa and the ordinate (c_{cf} only corrects the ordinate). Figure 5-3 of DNV-RP-F101 similarly corrects both the abscissa and the ordinate. The relative factor on the ordinate and on the abscissa is determined by the Folias factor. The Folias factor might over-estimate the stress concentration factor due to bulging, implying that the factor on the ordinate is too large and the factor on the abscissa is too small . That would be consistent with the trends in the full-scale test data, noting that the factor on the ordinate appears to be overly-conservative (the effective factor for $2c/(Rt)^{½}$ equal to 8.0 is higher than that in Annex D of BS ISO 27913 or in Figure 5-3 of DNV-RP-F104).

Figure 3b) includes the empirical correction factor due to Wilkowski et al., 1977 [31] (a more conservative correction factor than that due to Leis, 1997 & Eiber, 2008a,b [32-34]). A correction factor on the Charpy V-notch impact energy affects the abscissa; it does not affect the ordinate. A correction factor is appropriate because the impact energy of the line pipe in the nine full-scale tests is significantly higher than that in the original full-scale tests. The full-scale tests on liquid and dense phase CO_2 are conservatively predicted if Wilkowski et al., 1977 is used with an effective length equal to 8.0, but not if Leis, 1997 & Eiber, 2008a,b is used. The data points are conservatively predicted using the impact energy measured using a 2 or 8 mm striker (albeit most of the impact energies were measured using a 2 mm striker). Note that the full-scale tests are also all conservatively predicted if the higher estimated pressures at the crack tip in Table 3 of Michal et al., 2020 are used.

An effective length equal to 8.0 is, in the limit, more conservative than either Annex D of BS ISO 27913 or Figure 5-3 of DNV-RP-F104. It is less conservative than the "Possible boundary extension, no supporting test data" in Figure 3 of Michal et al. 2020.

An increase in the effective length is a relatively simple modification of the Two Curve Model. It is consistent with the full-scale test data, but it must be recognised that it is an approximation and that it might not be correct. A longer effective crack length represents a simple and, relative to Figure 5-3, a conservative alternative when Figure 5-3 is not applicable. A longer effective crack length does not, however, address the question of whether or not the assumptions that were made in the derivation of the Two Curve Model are appropriate. It also does not address the limitations of the Charpy V-notch test. It is a stepping-stone (or a blind alley). A revisiting and challenging of these assumptions will be required in order to move forward.

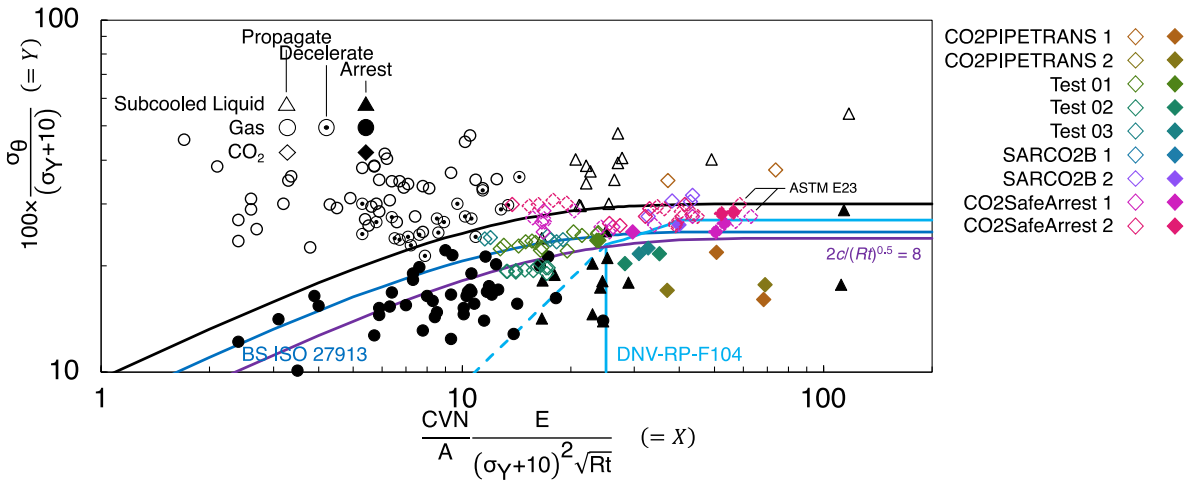

a) No correction factor

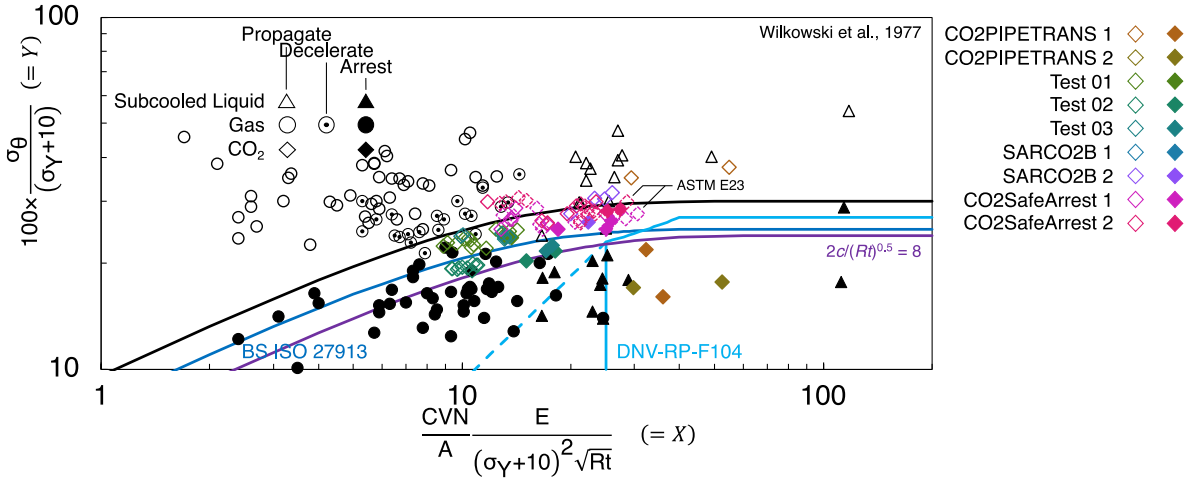

b) Wilkowski et al., 1977

Figure 3 A (re-)plot of the normalised decompressed stress level (=*Y*) versus the normalised toughness (=*X*) for the full-scale tests conducted with carbon dioxide, and an effective crack length, $2c/(Rt)^{0.5}$ equal to 8.0

5.6.5 *Procedure for evaluating ductile fracture propagation control* (Figure 5-3 and Table 5-5) of DNV-RP-F104 is not readily applicable to the repurposing of pipelines, because it requires a full-size equivalent Charpy V-notch impact energy that is greater than or equal to 250 J (see Table 5-5). It is also not applicable to smaller diameters, less than 16" (406.4 mm), or to lower grades, Grade L360 (X52) and below.

A pragmatic approach, albeit still somewhat arbitrary, would be to use, in order of preference: Figure 5-3 of DNV-RP-F104 within the limits defined in Table 5-5 (repeated in Table 3); and a modified form of the Two Curve Model, with an effective length equal to 8.0 and the correction factor due to Wilkowski et al., 1977. The modified form of the Two Curve Model also has limited experimental validation, but because it is directly based on the Two Curve Model, and is more conservative than the original model, it is considered to be applicable to a wider range of geometries and grades. Table 5-5 does not apply. Additional full-scale fracture propagation test data is required to validate this modified form of the Two Curve Model, or to extend Figure 5-3 of DNV-RP-F104.

Table 5-5 might be considered to be overly restrictive with respect to limiting the application of Figure 5-3 to welded line pipe with a submerged arc seam weld and fabricated using thermomechanical control processed steel. SARCO2B Test 2 included high frequency induction pipe. The arrest pipe was a high frequency induction pipe. CO2PipeTrans Tests 1 and 2 included high frequency induction and seamless pipes. The arrest pipes were a high frequency induction pipe and a seamless pipe, although as noted above, these tests do not bound the empirical model and the rig was relatively short. The limits in Table 5-5 should be reconsidered.

The modified form of the Two Curve Model should not be applied to grades that exceed Grade L450 (X65) or to diameters that exceed 914.4 mm (36"), the largest diameter and grade, respectively, in the set of full-scale tests on liquid and dense phase CO_2. It is more difficult to arrest a running ductile fracture in larger diameter than in smaller diameter pipe and in higher grade than in lower grade pipe. The modified form of the Two Curve Model should also not be used if the corrected full-size equivalent Charpy V-notch impact energy is greater than 200-250 J. The European Pipeline Research Group (EPRG) recommendations for crack arrest toughness for line pipe steel do not tabulate Charpy V-notch impact energies greater than 200 J, and note that a full-scale fracture propagation test is recommended if the calculated impact energy is greater than 200 J [35].

7. CONCLUSIONS

A reanalysis of the raw data for the full-scale tests conducted by COOLTRANS and CO2SafeArrest indicates that, on average, the data points for COOLTRANS Tests 01, 02 and 03 move down slightly and the data points for CO2SafeArrest Tests 1 and 2 move up slightly when re-plotted, but that Figure 5-3 of DNV-RP-F104 is still conservative.

Annex D of BS ISO 27913 is non-conservative.

A modified form of the Two Curve Model with a longer effective length, $2c/(Rt)^{½}$, equal to 8.0, and the correction factor due to Wilkowski et al, 1977 is shown to be conservative with respect to the full-scale test data. It is also more conservative than Figure 5-3 at higher values of the normalised toughness. It is considered to have wider applicability than Figure 5-3 of DNV-RP-F104 because it is based directly on, but is more conservative than, the Two Curve Model. It is, relative to Figure 5-3, a conservative alternative when Figure 5-3 is not applicable.

Additional full-scale fracture propagation test data is required to validate this modified form of the Two Curve Model, or to extend Figure 5-3 of DNV-RP-F104.

8. ACKNOWLEDGMENTS

The National Grid COOLTRANS project acknowledges the funding provided by the Don Valley CCS Project, co-financed by the European Union's European Energy Programme for Recovery. The CO2Safe-Arrest joint industry project acknowledges the funding provided by CLIMIT, Norway and the Department of Industry, Innovation and Science, Australia.

9. REFERENCES

1. DNV, 2021. Recommended Practice DNV-RP-F104 September 2021 Design and operation of carbon dioxide pipelines. Høvik, Norway: DNV GL.
2. Maxey, W.A., 1974. Fracture initiation, propagation and arrest. Paper J. In *Fifth Symposium on Line Pipe Research*. Houston, Texas, USA, 20-22 November 1974. Catalogue No. L30174. Chantilly, Virginia, USA: Pipeline Research Council International.
3. British Standards Institution, 2016. BS ISO 27913:2016 Carbon Dioxide Capture, Transportation and Geological Storage – Pipeline transportation systems. London, UK: British Standards Institution.
4. Maxey, W.A., Kiefner, J.F., Eiber, R.J. and Duffy, A.R., 1972. Ductile fracture initiation, propagation, and arrest in cylindrical vessels. In *Fracture Toughness. Proceedings of the 1971 National Symposium on Fracture Mechanics Part II*. ASTM STP 514. Urbana-Champaign, Illinois, 31 August-2 September 1971. Philadelphia, USA: American Society for Testing and Materials. 70-81.
5. Maxey, W.A., Kiefner, J.F., Eiber, R.J. and Duffy, A.R., 1973. Experimental investigation of ductile fractures in piping. Paper No. IGU/C 34-73, In *Proceedings of the 12th World Gas Conference*. Nice, France, 4-6 June 1973. London, UK: International Gas Union.
6. King, G.G., 1982. CO_2 Pipeline Design–1 Here are key design considerations for CO_2 pipelines. In *Oil & Gas Journal*, 80(39): 219-222.
7. King, G.G., 1982. CO_2 Pipeline Design–Conclusions Propagating fractures, pipe sizing probed for high-operating-pressure CO_2 pipelines. In *Oil & Gas Journal*, 80(40): 100-102.
8. Maxey, W.A., 1986. Long shear fractures in CO_2 lines controlled by regulating saturation, arrest pressures. In *Oil and Gas Journal*, 84(31): 44-46.
9. Rothwell, A.B., 1988. Fracture control in natural gas and CO_2 pipelines. In *Microalloyed HSLA Steels. Proceedings of Microalloying '88 Held in Conjunction with the 1988 World Materials Congress*. Chicago, Illinois, USA, 24-30 September 1988. Metals Park, OH, USA: ASM International. 95-108.
10. Folias, E.S., 1965. An axial crack in a pressurized cylindrical shell. In *International Journal of Fracture Mechanics*, 1(1): 104-113.
11. Erdogan, F. and Kibler, J.J., 1969. Cylindrical and spherical shells with cracks. In *International Journal of Fracture Mechanics*, 5(3): 229-237.
12. Hahn, G.T., Sarrate, M. and Rosenfield, A.R., 1969. Criteria for crack extension in cylindrical pressure vessels. In *International Journal of Fracture Mechanics*, 5(3): 187-210.
13. Bilby, B.A., Cottrell, A.H. and Swinden, K.H., 1963. The spread of plastic yield from a notch. In *Proceedings of the Royal Society of London. Series A, Mathematical and Physical Sciences*, A272(1350): 304-314.
14. Heald, P.T., Spink, G.M. and Worthington, P.J., 1972. Post yield fracture mechanics. In *Materials Science and Engineering*, 10: 129-138.
15. Røneid, S. and Bubenik, T.A., 2014. Fracture arrest testing of CO2 pipelines. In *37th Annual Offshore Pipeline Technology (OPT) Conference*. OPT 2014. Amsterdam, The Netherlands, 26-27 February 2014. London, UK: IBC Energy.
16. Aursand, E., Dumoulin, S., Hammer, M., Lange, H.I., Morin, A., Munkejord, S.T. and Nordhagen, H.O., 2016. Fracture propagation control in CO2 pipelines: Validation of a coupled fluid-structure model, In *Engineering Structures*, 123 (2016): 192-212.
17. Cosham, A., Jones, D.G., Armstrong, K., Allason, D. and Barnett, J., 2014. Analysis of two dense phase carbon dioxide full-scale fracture propagation tests. Paper No. IPC2014-33080. In *Proceedings of the 2014 10th International Pipeline Conference*. IPC2014. Calgary, Alberta, Canada, 29 September-3 October 2014. New York, NY, USA: American Society of Mechanical Engineers.
18. Cosham, A., Jones, D.G., Armstrong, K., Allason, D. and Barnett, J., 2016. Analysis of a dense phase carbon dioxide full-scale fracture propagation test in 24 inch diameter pipe. Paper No. IPC2016-64456. In *Proceedings of the 2016 11th International Pipeline Conference*. IPC2016. Calgary, Alberta, Canada, 26-30 September 2016. New York, NY, USA: American Society of Mechanical Engineers.
19. Di Biagio, M., Demofonti, G., Lucci A. and Spinelli, C.M., 2015. Research Fund for Coal & Steel SARCO2 Project, Full scale fracture propagation testing on dense phase CO2 pipeline. Paper 6. In *EPRG/PRCI/APGA-RSC 20th Joint Technical Meeting on Pipeline Research*. Paris, France, 3-8 May 2015. Duisburg, Germany: European Pipeline Research Group.

20. Di Biagio, M. Lucci, A., Mecozzi, E. and Spinelli, C.M., 2017. Fracture propagation prevention on CO_2 pipelines: Full scale experimental testing and verification approach. Paper 28. In *21st PRCI-APGA-EPRG Joint Technical Meeting on Pipeline Research*. Colorado Springs, Colorado, USA, 1-5 May 2017. Arlington, Virginia, USA: Pipeline Research Council International.
21. Di Biagio, M. Lucci, A., Mecozzi, E. and Spinelli, C.M., 2017. Fracture propagation prevention on CO_2 pipelines: Full scale experimental testing and verification approach. In *17th Pipeline Technology Conference*. Berlin, Germany, 2-4 May 2017. Hannover, Germany: EITEP Institute.
22. Linton, V., Leinum, B.H., Newton R. and Fyrileiv, O., 2018. CO2SAFE-ARREST: A full-scale burst test research program for carbon dioxide pipelines – Part 1: Project overview and outcomes of Test 1. Paper No. IPC2018-78517. In *Proceedings of the 2018 12th International Pipeline Conference*. IPC2018. Calgary, Alberta, Canada, 24-28 September 2018. New York, NY, USA: American Society of Mechanical Engineers.
23. Michal, G., Davis, B.J., Østby, E., Lu, C. and Røneid, S., 2018. CO2SAFE-ARREST: A full-scale burst test research program for carbon dioxide pipelines – Part 2: Is the BTCM out of touch with dense-phase CO_2? Paper No. IPC2018-78525. In *Proceedings of the 2018 12th International Pipeline Conference*. IPC2018. Calgary, Alberta, Canada, 24-28 September 2018. New York, NY, USA: American Society of Mechanical Engineers.
24. Michal, G., Davis, B.J., Lu, C. and Linton, V., 2019. Effect of backfill in a dense-phase CO_2 full-scale fracture propagation test. Paper 29. In *APGA-EPRG-PRCI 22nd Joint Technical Meeting on Pipeline Research*. Brisbane, Australia, 29 April-3 May 2019. Kingston, ACT, Australia: Australian Pipelines and Gas Association.
25. Michal, G., Øtsby, E., Davis, B.J., Røneid, S. and Lu, C., 2020. An empirical fracture control model for dense-phase CO_2 carrying pipelines. Paper No. IPC2020-9421. In *Proceedings of the 2020 13th International Pipeline Conference*. IPC2020. Calgary, Alberta, Canada, 28-30 September 2020. New York, NY, USA: American Society of Mechanical Engineers.
26. Maxey, W.A., 1983. *Gas expansion studies*. NG-18 Report No. 133. Catalogue No. L51435. Falls Church, VA, USA: Pipeline Research Council International.
27. Wilkowski, G., Rudland, D. and Rothwell, B., 2006. How to optimize the design of mechanical crack arrestors. Paper No. IPC2006-10357. In *Proceedings of IPC2006 2006 International Pipeline Conference*. Calgary, Alberta, Canada, September 25-29, 2006. New York, NY, USA: American Society of Mechanical Engineers.
28. Ahluwalia, K.S. and Gupta, G.D., 1985. Composite Reinforced Pipelines. Paper H3. In *6th International Conference on the Internal and External Protection of Pipes*. Nice, France, 5-7 November 1985. BHRA, Cranfield, UK. 341-351.
29. American Society for Testing and Materials, 2018. *ASTM E23-18 Standard Test Methods for Notched Bar Impact Testing of Metallic Materials*. West Conshohocken, Pennsylvania, USA: ASTM International.
30. British Standards Institution, 2016. BS EN ISO 148-1:2016 Metallic materials – Charpy pendulum impact test. Part 1: Test method. London, UK: British Standards Institution.
31. Wilkowski, G.M., Maxey, W.A. and Eiber, R.J., 1977. Use of a brittle notch DWTT specimen to predict fracture characteristics of line pipe steels. Paper No. 77-Pet-21. In *Energy Technology Conference*. Houston, Texas, USA, 18-22 September 1977. New York, NY, USA: American Society of Mechanical Engineers.
32. Leis, B.N., 1997. *Relationship between apparent (total) Charpy Vee-Notch toughness and the corresponding dynamic crack-propagation resistance*. Columbus, Ohio, USA: Battelle Memorial Institute. [online] Available at: <https://docs.neb-one.gc.ca/ll-eng/llisapi.dll?func=llworkspace> 98-06-10 NEB - GH-3-97 Exhibit List (A13687). A0W3T3 - B - Alliance Pipeline Ltd. Exhibit No. B-82 & Exhibit No. B-114.
33. Eiber, R.J., 2008. Fracture Propagation – 1: Fracture-arrest prediction requires correction factors. In *Oil & Gas Journal*, 106(39).
34. Eiber, R.J., 2008. Fracture Propagation – Conclusion: Prediction steel grade dependent. In *Oil & Gas Journal*, 106(40).

35. Cosham, A., Andrews, R.M. and Schmidt, T., 2018. The EPRG recommendations for crack arrest toughness for line pipe steel. Paper No. IPC2018-78043. In *Proceedings of the 2018 12th International Pipeline Conference*. IPC2018. Calgary, Alberta, Canada, 24-28 September 2018. New York, NY, USA: American Society of Mechanical Engineers.